



Reservoir Characterization of the NKO Field, Onshore Niger Delta Basin Using Multi-Seismic Attribute Algorithms

Omezi Ifeanyi and C.C. Ezeh

Department of Petroleum Engineering, Nnamdi Azikiwe University, Awka, Nigeria

DOI: https://dx.doi.org/10.51584/IJRIAS.2025.10100000136

Received: 20 October 2025; Accepted: 26 October 2025; Published: 15 November 2025

INTRODUCTION

The use of seismic attributes derived from seismic data has received considerable attention in reservoir characterization, especially in defining reservoir properties, and offers reliable solutions to the perceived reservoir problems within an old producing field (Ahaneku et al., 2016; Nwaezeapu et al., 2017; Obiadi et al., 2019). The seismic data also presents information related to stratigraphic features, rock property changes, and hydrocarbon accumulations. Seismic amplitudes which represent primarily contrast in elastic properties between individual layers contain information about lithology, porosity, pore fluid type, and saturation – information that cannot be gained without integrating seismic attributes, well log, and 3-D structural interpretation. The use of seismic attributes has proven to be one of the best techniques for quantitative seismic interpretation as the method can validate hydrocarbon anomalies and give valuable information during prospect evaluation, reservoir characterization, and production simulation (Taner et al., 1979).

In seismic surveys, employing reflection and refraction techniques, provide detailed images of the subsurface, aiding in identifying structural traps, stratigraphic features, and fluid contacts within the reservoir (Owen, 2024). Advanced techniques in reservoir characterization include 3D and 4D seismic imaging. 3D seismic provides a three-dimensional view of the reservoir, enhancing the understanding of its structure and stratigraphy, and is crucial for identifying subtle features and heterogeneities within the reservoir. 4D seismic, also known as time-lapse seismic, monitors changes in the reservoir over time, providing insights into fluid movement and reservoir dynamics during production.

Various interpretation techniques have been released on the use of seismic amplitude in characterizing reservoirs. These include seismic attribute analysis and Amplitude-Variation-with -Offset (AVO). In the early 1970s, large reflection amplitudes such as "bright spots" were known as potential hydrocarbon indicators. Adding hydrocarbons to a porous sand unit generally influences the reservoir's acoustic impedance relative to the surrounding formations, thus causing bright spots or any kind of amplitude anomalies. However, as efficient as these techniques were, they have accounted for numerous abandoned wells. Recent studies have confirmed that bright spots may also be caused by the presence of unusual lithologies, such as over-pressured shale and coal (Sen, 2006). Hence, there is a need to critically analyze what actually influences the seismic response (seismic amplitude) before interpretation. In order to accomplish this task, a rock-property model that relates the petrophysical properties to the seismic rock properties has to be established.

This study aims to carry out a reservoir characterization of NKO field, onshore Niger Delta Basin using multiseismic Attribute Algorithms. The aim of the study will be achieved through the following objectives: delineating the lithofacies stratigraphic framework using well-logs, characterizing the reservoirs and evaluate their petrophysical properties, build a robust structural and tectonostratigraphic framework of the NKO Field well-log and seismic data, generate volume and surface attributes for prospect identification and analysis.

Location of the Study Area

The study area is located onshore within the southeastern Central Swamp Depobelt, Niger Delta Basin, Nigeria. It lies between Longitudes 5° 50' E and 6° 13' E, and Latitudes 5° 54' N and 6° 04' N. The field was discovered in 1996 by a multinational operating in Nigeria and till date only Fifty-seven wells have been drilled in the field. The 3-D seismic data covered at least an area of 89 km². The bin spacing of the data should be within 25.00m (inline) by 25.00m (cross-line), a sample rate of 2 milliseconds, and a record length of 6000 milliseconds Two-Way-Time (TWT ms). The data is stored in SEG-Y format and has a zero phase SEG

ISSN No. 2454-6194 | DOI: 10.51584/IJRIAS | Volume X Issue X October 2025



(reverse) polarity where a peak represents the positive amplitude (reflectivity) or increasing acoustic impedance coloured red, and a trough represents the negative amplitude (reflectivity) or decreasing acoustic impedance coloured blue (Figure 3.1). The in-line (dip section) ranges from 11600 - 13300, while the crossline (strike section) ranges from 3300 – 4000. The amplitude ranges from -33024 to 32766, with a dominant frequency of 22Hz.

General Overview of the Niger Delta Basin

The Niger Delta is situated on the continental margin of the South Atlantic within the Gulf of Guinea in West Africa, between Latitudes 3° and 6° N and longitudes 5° and 8° E (Reijer et al., 1997). It ranks amongst the world's most prolific petroleum-producing Tertiary deltas account for about 5% of the world's oil and gas reserves (Aniefiok et al., 2013). The Benin Flank marks the western limit of the basin. Cretaceous sediments of the Anambra and the Abakaliki Basins define the northern boundary, while the Calabar Hingeline marks the eastern limits (Reijers et al., 1997). The basin stretches for about 300 km from the apex to the mouth and covers an area of about 70,000 km² (Doust & Omatsola, 1990).

Structural Patterns of the Niger Delta Basin

The Tertiary Niger Delta is characterized by syn-sedimentary gravitational growth faults, developed as a result of rapid sand deposition and differential loading of coarser clastic over fine-grained under-compacted marine shales of the Akata Formation (Ajakaiye & Bally, 2002). Evamy et al. (1978) described the fault types commonly found in the Niger Delta Basin, including normal growth faults, down-to-basin listric normal faults, synthetic and antithetic normal faults, rollover anticlines and diapirs. The growth faults are contemporaneous and more or less continuously active with deposition, so their throws increase with depth.

Review of Related Works

Seismic attributes play a crucial role in reservoir characterization, aiding in identifying key geological features. Attributes such as reflection intensity, sweetness, variance, envelope, instantaneous frequency, time gain, trace AGC, local structural dip, gradient magnitude, and RMS amplitude are commonly used to extract valuable information from seismic data for reservoir evaluation (Amit et al., 2023; Sofolabo & Nwakanma, 2022). These attributes help in mapping out faults, fractures, lithology changes, and potential hydrocarbon zones within the reservoir, enhancing the understanding of subsurface geological features and fluid distribution (Sofolabo & Nwakanma, 2022). Additionally, attributes like intercept and gradient in AVO analysis are utilized to map reservoir properties such as lithology, porosity, and fluid saturation, contributing to quantitative reservoir characterization (Kumar, 2023). Incorporating unsupervised machine learning techniques like Self-Organizing Maps (SOM) further refines the interpretation of seismic attributes, enabling the delineation of fault-fracture networks and guiding natural fracture network propagation in naturally fractured reservoirs (Amit et al., 2023).

Ali and Rahim (2022) applied seismic attributes in characterizing natural gas reservoirs, highlighting key indicators such as bright spots, flat spots, and polarity changes that aid in gas detection. Their research emphasized the integration of seismic data with core and well-log information to enhance the mapping of rock and fluid properties, thereby reducing uncertainty in reservoir models. Also, the research discusses the use of statistics as well as the use of machine learning techniques to formulate relationships between seismic attributes and reservoir characteristics, providing practical case studies that illustrate their effectiveness in exploration and development efforts.

Anderson & Pedro (2021) presented an integrated approach for characterizing reservoirs, focusing on a case study from the Barreirinhas basin in Maranhão, Brazil. It emphasizes the usefulness of combining various geological and geophysical data, for instance seismic attributes, used to improve the understanding of reservoir properties and enhance gas detection. The study demonstrates how this integrated methodology can lead to more accurate reservoir models and better decision-making in exploration and production activities.

A literature review regarding the use of seismic attributes in the characterization of hydrocarbon reservoirs has been presented by Oumarou et al. (2021). The research aims to identify and classify various seismic attributes, such as instantaneous frequencies, based on their effectiveness in analyzing hydrocarbon accumulation zones.



The paper also discusses the limitations of existing seismic attributes and seeks to explore new attributes that have not been previously utilized in reservoir analysis. Ultimately, the work aims to enhance the understanding of reservoir characterization by evaluating the strengths and weaknesses of different seismic attributes.

Nyeneime *et al.* (2020) evaluated a number of seismic attributes over the Edi field in the Niger Delta, Nigeria, using 3D seismic data to enhance reservoir characterization.

METHODOLOGY

The reservoir characterization of the NKO field in the Central Swamp Depobelt, Niger Delta Basin, Nigeria, was interpreted using 3-D seismic data and 32 well logs. The well-logs and seismic data will be interpreted using petrel interpretation software. The packages used include all available seismic fig 1 and well data interpretation tools.

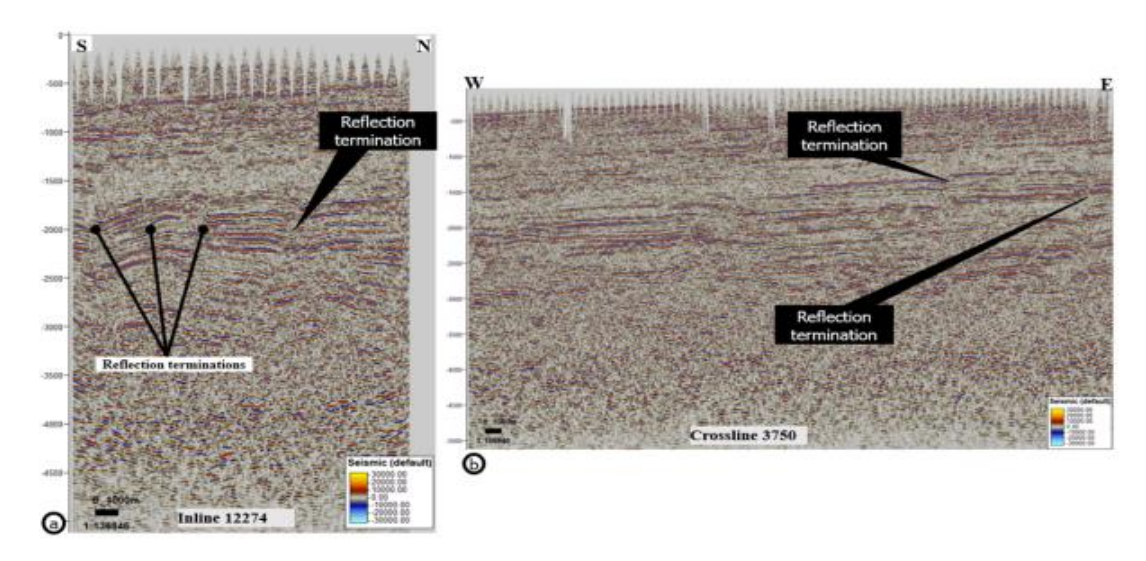


Figure 1: Showing the seismic reflection data quality

The Petrel software was used to carry out a detailed well-log interpretation, petrophysical analysis, and seismic data interpretation, generate synthetic seismogram, and construct maps. The data set were quality checked before loading into Petrel and arranged in formats readable by Petrel.

A multi-attribute seismic analysis was carried out to increase the reliability of the subsurface predictions. Well-log cross-sections and corresponding seismic transects through the 3-D volume were interpreted throughout the area to present the structural framework of the Field. Seismic attributes were studied to enhance signal-to-noise ratio of the seismic data, enhance the visibility of the faults, evaluate direct hydrocarbon indicators (DHIs) and characterize potential reservoirs at deeper levels. Petrophysical analysis was carried out to evaluate the quality of the reservoirs.

A synthetic seismogram which simulated seismic response computed from well data. It correlated geological data from well-logs recorded depth (meters or feet) with geophysical data from seismic recorded time. This was done by using check-shot data to correct the sonic log (representing velocity) multiplied by the density log to generate the acoustic impedance and reflectivity series. The reflectivity series is then convolved using a zero-phased wavelet extracted from the seismic data.

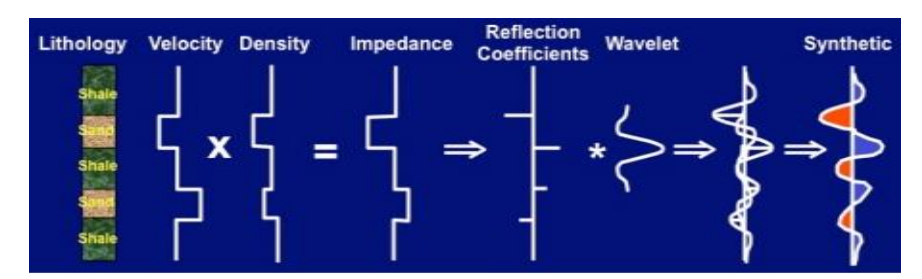


Figure 2: Synthetic seismogram generation model using density and sonic log (Shell, 2017).

Seismic Attribute Analysis

Proper interpretation of faults and horizons is very important in seismic interpretation for the purpose of modelling the structure and stratigraphy of hydrocarbon reservoirs and field development (Ahaneku et al., 2016). Signal-processing and edge-detection attributes were applied to the original seismic volume which help in the visualization and interpretation of the fault networks and hydrocarbon-bearing reservoirs associated with bright spots within the study area. These attributes objectively translate the seismic data into a geologically meaningful image.

The Variance (edge) attribute was applied to the original seismic data to interpret the faults within the study area. For consistency, the variance (edge) attribute and the original seismic will be compared, and the faulting systems within the field will be better highlighted in the variance (edge) attribute volume. The spatial visualization of semblance attributes on time slices allows for a better understanding of the distribution of faults within the study area (Figure 4).

Seismic attributes have nowadays become an important tool in seismic interpretation techniques. The interpretation of structural and stratigraphic features has thereby improved. For delineating subtle features like faults and stratigraphic features like channels and analyzing the amplitude spectra of the seismic data, spectral decomposition tool proves to be a better technique within the seismic data. The output of this decomposition is referred to as a tuning cube which is thoroughly investigated for identifying the tuning frequency that best resolves these geological features. After analysis of the amplitude spectrum of the seismic data, spectral decomposition technique is applied. This spectrum (Fig 3) helps to identify different frequency zones like low frequency zone (10Hz to 20Hz), mid frequency zone (25Hz to 40 Hz) and high frequency zone (45Hz to 60 Hz) which are used for decomposing the seismic data volume.

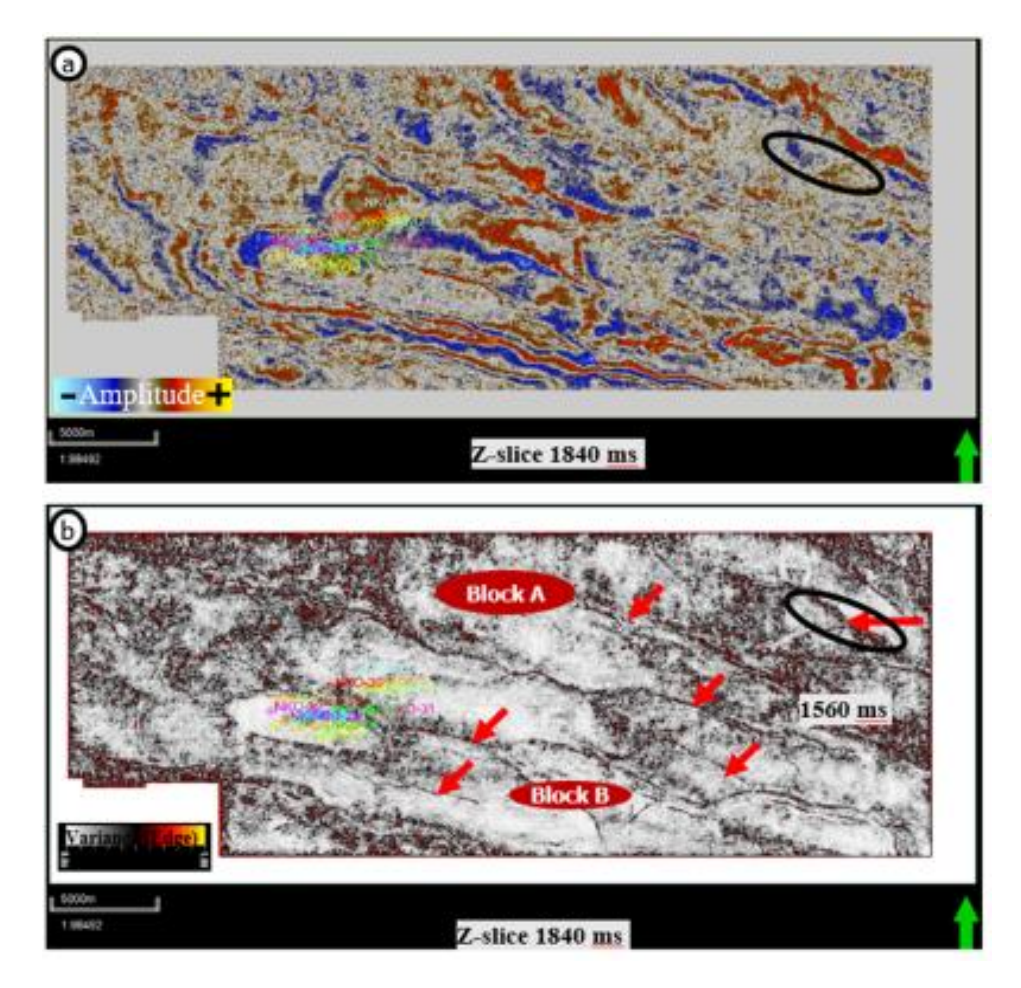


Figure 3: An example of (a). Original seismic data and (b). Variance (edge) attribute at Z-slice 1840ms.

The variance (edge) attribute clearly shows the faults within the field that were not evident in the original seismic data.

RESULTS AND INTERPRETATION

Petrophysical Analysis of Well Logs for Reservoir Evaluation

Accurate interpretation of well logs in essential for reservoir evaluation and characterization. Log correlation provides the foundation for determining the geometry and architecture of reservoirs, enabling a comprehensive understanding of the subsurface geology.

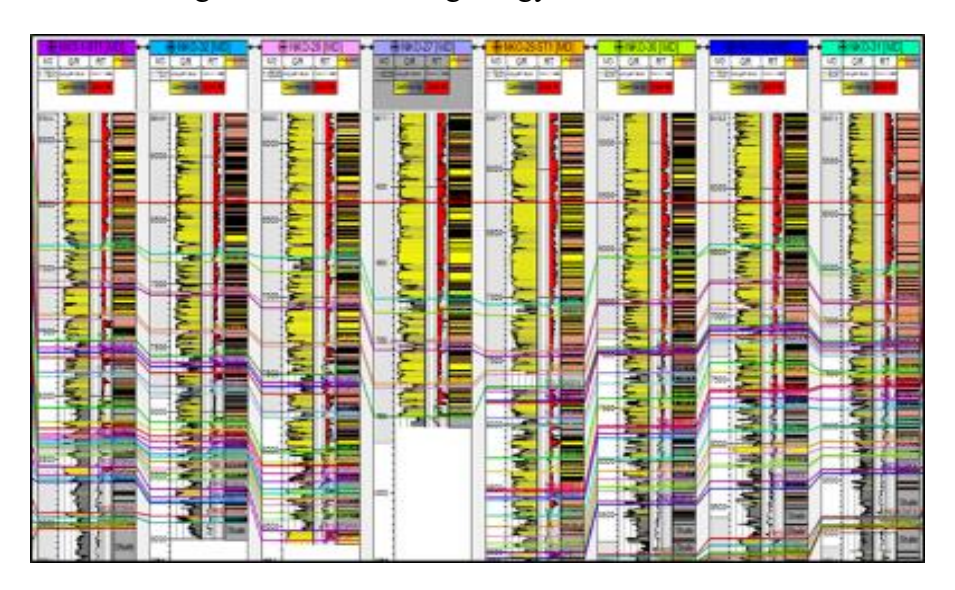


Figure 4: Well Log Correlation across the wells

A comprehensive petrophysical properties analysis was performed on the wells to investigate the quality of the reservoirs rock. The analysis focused on key petrophysical parameters, including volume of shale, net-to-gross volume, porosity, permeability, water saturation and hydrocarbon saturation.

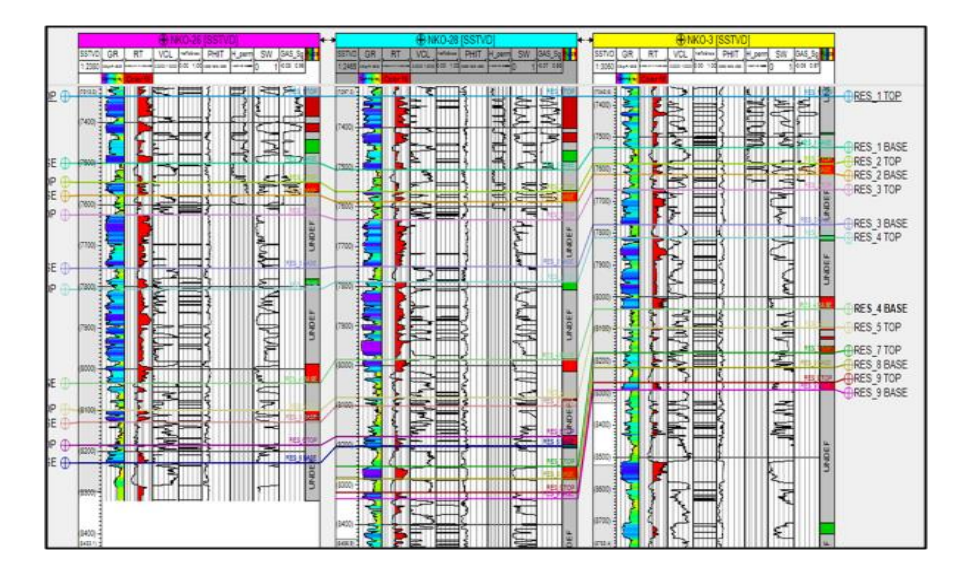


Figure 5: Showing Petrophysical Properties along The Vertical Section of the Study Area Penetrated by the Wells

Res 2 Reservoir Interval

The Res_2 reservoir interval was similarly penetrated by all 32 wells, providing a comprehensive dataset for analysis. Further subdivision of the reservoir into two distinct intervals, designated as Res_2A and Res_2B, is clearly illustrated in Figure 6, enabling a more nuanced understanding of the reservoir's internal architecture. The estimated average petrophysical properties of these intervals, including key parameters such as porosity, permeability, and water saturation, are succinctly summarized in Table 1, offering valuable insights into the reservoir's potential hydrocarbon-bearing capabilities and informing future development strategies.



Figure 6: Res 2 Reservoir Interval across Wells

The Res_2 reservoir interval exhibits a total porosity range of 0.24 to 0.32, indicating a moderate to good storage capacity, while the effective porosity, which is a critical parameter for hydrocarbon flow, was computed to range from 0.22 to 0.29, suggesting a potentially significant proportion of interconnected pore spaces. The volume of shale within the Res_2 reservoir interval varies between 0.12 and 0.23, which is relatively consistent with the lithology expected in this geological setting, and the net-to-gross ratio ranges from 0.75 to 0.89, indicating a relatively high proportion of reservoir-quality rock. Permeability, a key factor controlling fluid flow, ranges from 589mD to 987mD, suggesting a moderate to good flow potential. Hydrocarbon saturation within the Res_2 reservoir interval is estimated to range from 0.62 to 0.71, indicating a significant presence of hydrocarbons and potentially commercial quantities.

Table 1: Average Petrophysical of RES_2 Reservoir Interval

Wells	V_{sh}	NTG	PE	Perm	Sh
Nko_27	0.21	0.79	0.24	658	0.69
Nko_28	0.12	0.88	0.26	953	0.62
Nko_29	0.18	0.82	0.22	753	0.67
Nok_31	0.25	0.75	0.25	856	0.70
Nko_1	0.11	0.89	0.29	987	0.63
Nko_32	0.19	0.81	0.24	786	0.67
Nko_12	0.23	0.77	0.27	658	0.71
Nko_30	0.21	0.89	0.23	589	0.65

Seismic-Well Tie

Following the well correlation, a sonic calibration was performed to integrate the accuracy of the checkshot data with the sonic log's detailed information, resulting in an optimized time-depth relationship (TDR) as shown in Figure 7 below. This updated TDR was then applied to the well, enabling accurate synthetic generation and successful seismic data correlation for well Nko_31. A zero-phase 25 Hz Ricker wavelet with normal polarity was used for the convolution (Figures 8 and 9). The wavelet frequency was estimated from seismic data within the reservoirs of interest. The zero-phase 25 Hz Ricker wavelet was selected based on accompanying dataset information indicating that the seismic data is zero-phase. The synthetic generation involves calculating acoustic impedance by multiplying sonic and density logs. The acoustic impedance is then used to compute the reflection coefficient, which is then convolved with a 25 Hz Ricker wavelet to produce a synthetic seismogram. A good correlation was achieved after applying a bulk shift of -12 ms to align the synthetic with the seismic data as depicted in Figures 8, 9, and 10 below. This shift was necessary to match the geological response between the seismic data and the seismogram (Figure 9). The well tie analysis reveals that



the top of the targeted reservoirs corresponds to the peak, indicating that they are consisting of high-impedance sands overlain by low-impedance shale layers (Figures 9 and 10). Following the successful well tie for well Nko_31, the remaining wells were tied to the seismic data, revealing consistent polarity across all wells with chechshot data within the targeted reservoirs.

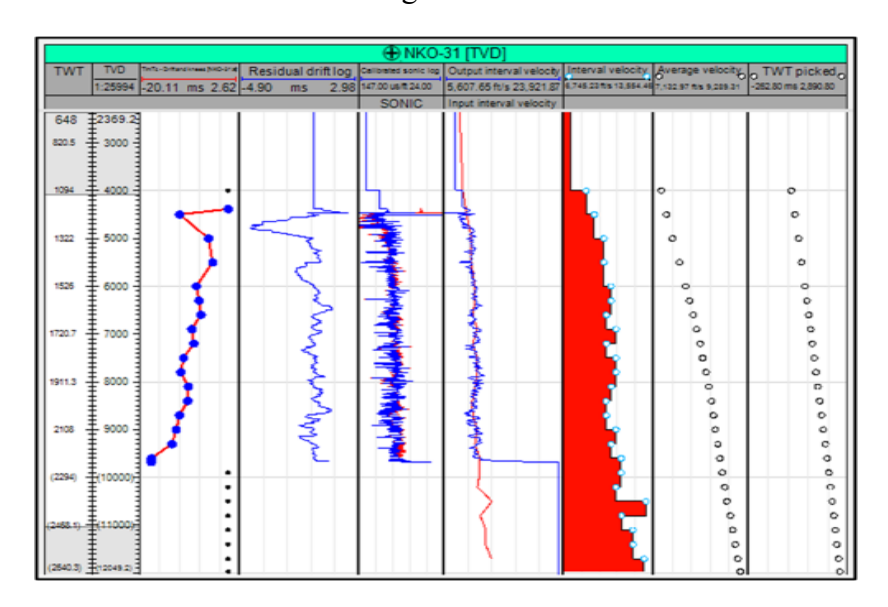


Figure 7: Well Log Sonic Calibration of Nko_31

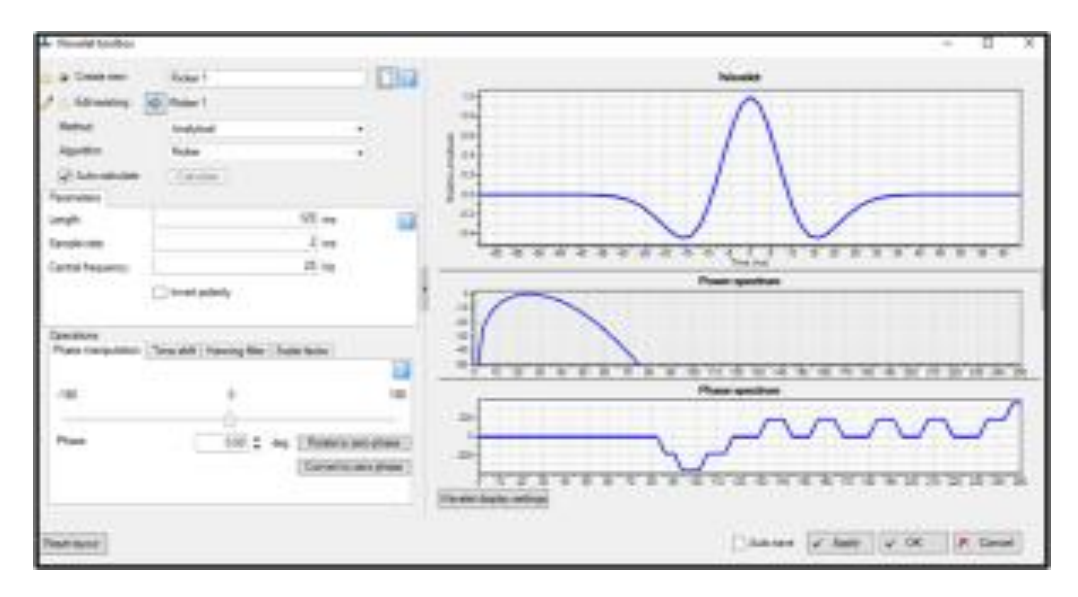


Figure 8: Tool Box for Generating Synthetic Seismogram

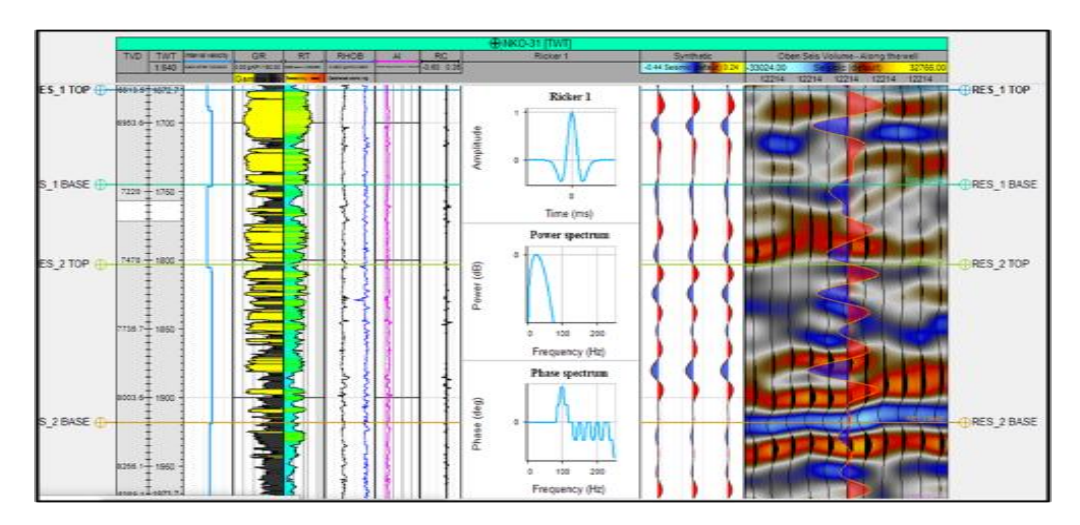


Figure 9: synthetic seismogram for well nko_31

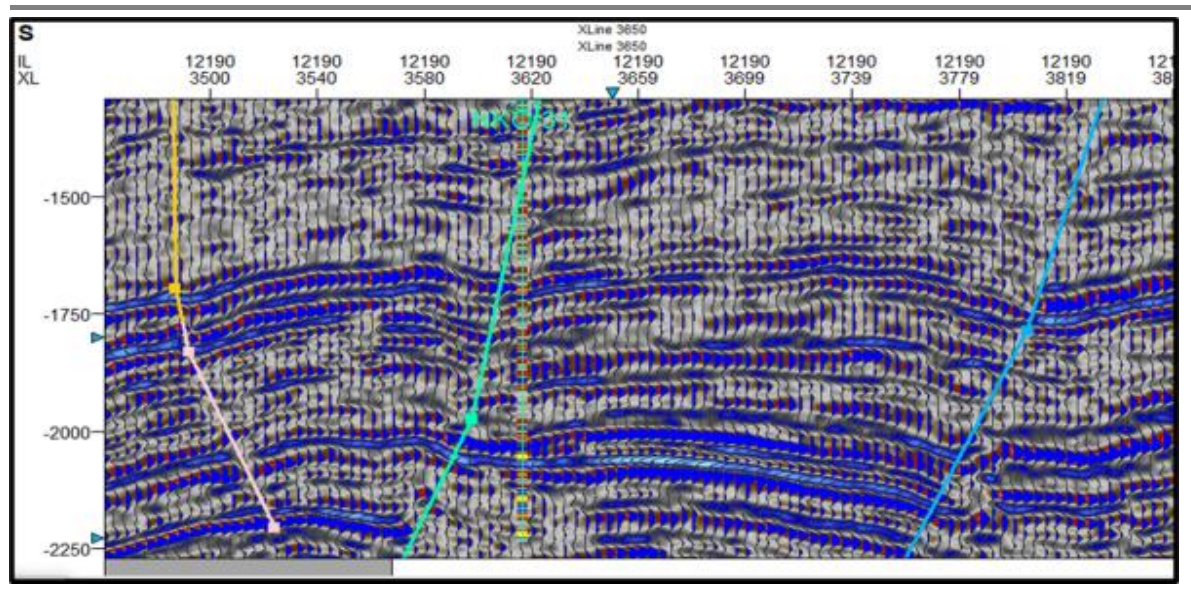


Figure 10: Correlation of Synthetic and Seismic Data

Structural and Stratigraphic Framework

The 3D Nko seismic cube has 1701 in-lines and 701 cross-lines. Both the inlines and the crossline have intervals of 25. The seismic has a sample interval of 4, number of samples per trace is 1501, number of cells total is 1789783901, inline length is 17500 and crossline length is 42500. The seismic line provides information of up to 6000 ms two-way travel time (TWT) with our horizons of interest lying between a time interval of 2571 ms and 1031 ms (Figure 11). Interpretation challenges arose due to the poor resolution and continuity of the reflectors at a depth of about 2571 ms TWT. To address this problem, both the inlines and crosslines were analyzed with a 10-unit intersection interval, enhancing the understanding of the region. Only the horizons of interest, that is Res 1 to Res 6 were identified and interpreted, together with the structures that influenced the horizons like faults (Figures 11, and 12). These six horizons were first identified on well logs and then superimposed on seismic using checkshot data. That is, the identified sand bearing zones were then tie to specific reflectors on the seismic data and interpreted as reservoir horizons. The fault activities not only cause deformation of the basin but also influence the migration and trapping of hydrocarbon. Fault interpretation is therefore a critical component of structural modeling. A total of 42 faults were identified and mapped, with three major faults causing significant displacement in the region. These faults were identified based on breaks in the reflection, distortion in amplitude around a fault zone, and sudden termination of reflection events (changes in the dip of an event). The interpreted faults exhibited a consistent pattern across the entire seismic data with growth fault (listric) dipping basinward away from the direction of sediment supply, antithetic (landward direction of the fault plane) (Figure 12). Fault orientations were linked to the tectonic episodes to show how these affected their architecture and role in the trapping and migration of hydrocarbon. Two categories of fault have been identified based on their orientation; category I and category II.

Category I: This category of faults has azimuth in the NE-SW direction as shown in (Figure 12) below. These faults have been observed dipping both basinward and landward, however a predominant trend of dipping basinward has been identifies as shown in (Figure 13) below. The major bounding faults with listric geometries form the main depobelts, graben in the field (Figure 13). Although the major affects the entire succession of sediments, no evidence of major activity of deposition have been observed. The thickness of sediments across the faults of Category I varies. Nevertheless, this variation in thickness observed is related to the geometry of the region and as well were majorly structurally controlled. The major fault are syn-depositional fault and form rotate fault-blocks

Category II: They have a NW-SE orientation (Figures 12 and 13) normal fault without any indication of listric geometry. These faults are mainly collapse crest, and minor relay faults and serve as seals and migrating path (leaks) at different places. Therefore, a throw map will be imperative to determine and show the variation of throw displacement along the fault. Therefore, these faults indicate there were no major tectonic activity at the

time the sediments were deposited. The thickness across the faults appears constant. Therefore, the structural activity in the region affected sedimentary process, creating an interplay of faulting, and zones of collapse crest faults.

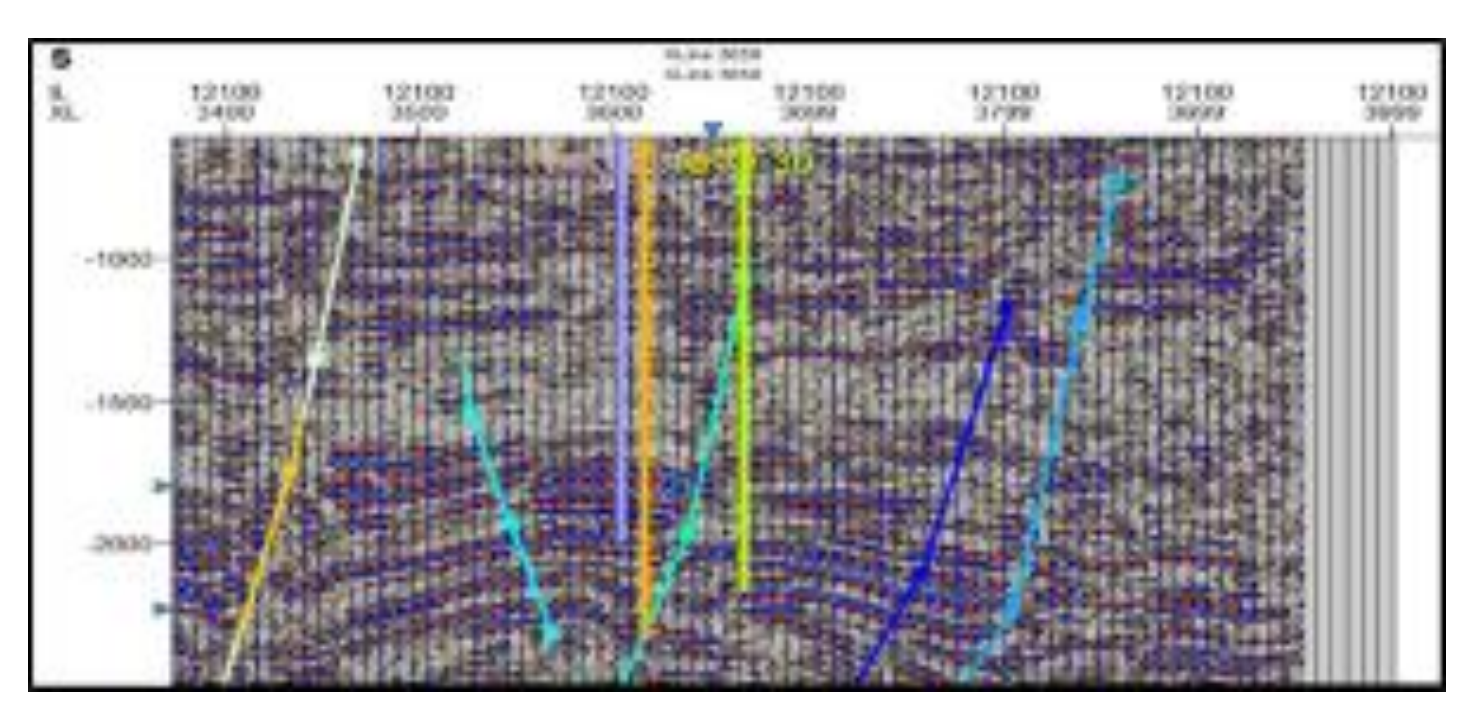


Figure 11: Displaying Wells on Seismic Data

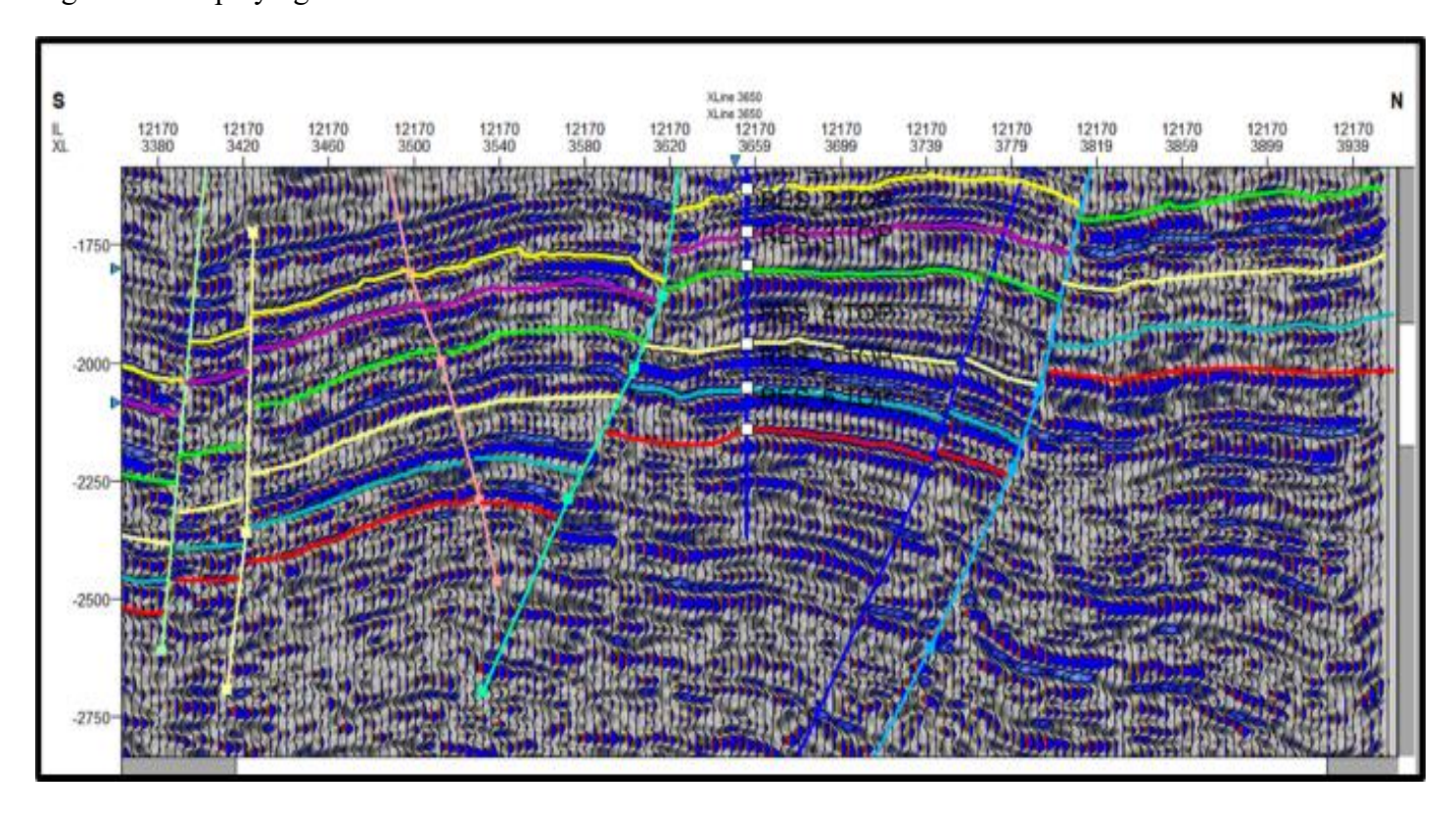


Figure 12: Displaying Interpreted Horizon, Faults and Well on Inline 12170

Seismic Volume Attribute Analysis

Generally, seismic attributes provide both quantitative and qualitative insights that describe the relationship between seismic responses and the underlying geologic feature. For this study, the attribute selected were based on their ability to enhance features from the geologic model that were not readily apparent in the original seismic data. Specifically, the targeted characteristics include stratigraphic elements, faults, and channels (mass transport complexes). The selected volume attributes use for this study include RMS amplitude, variance-edge,



sweetness attributes, dip and curvature (Figures 14, 15 16, 17, 18, 19, 20, 21, 22). To understand the cause of amplitude variations, seismic attributes were quantitatively examined across various seismic inline and time slice. These attributes were selected due to their relevance to hydrocarbon and the ability to highlight structural and stratigraphic features.

A cross section through well Nko_31 ST1 reveals that reservoir RES_2 contain hydrocarbon (Figure 14). However, well Nko_31 encountered brine in another reservoir, consistent with the earlier finding from the seismic-to-well tie, the tops of the reservoirs correspond to the peaks. On inline 12210, it was observed that the tops of both the hydrocarbon bearing sand and non-hydrocarbon bearing sand intervals correlate to the seismic peak (Figure 14 below). High values of RMS amplitude were associated to high porous lithologies, which are potential hydrocarbon bearing reservoir sands.

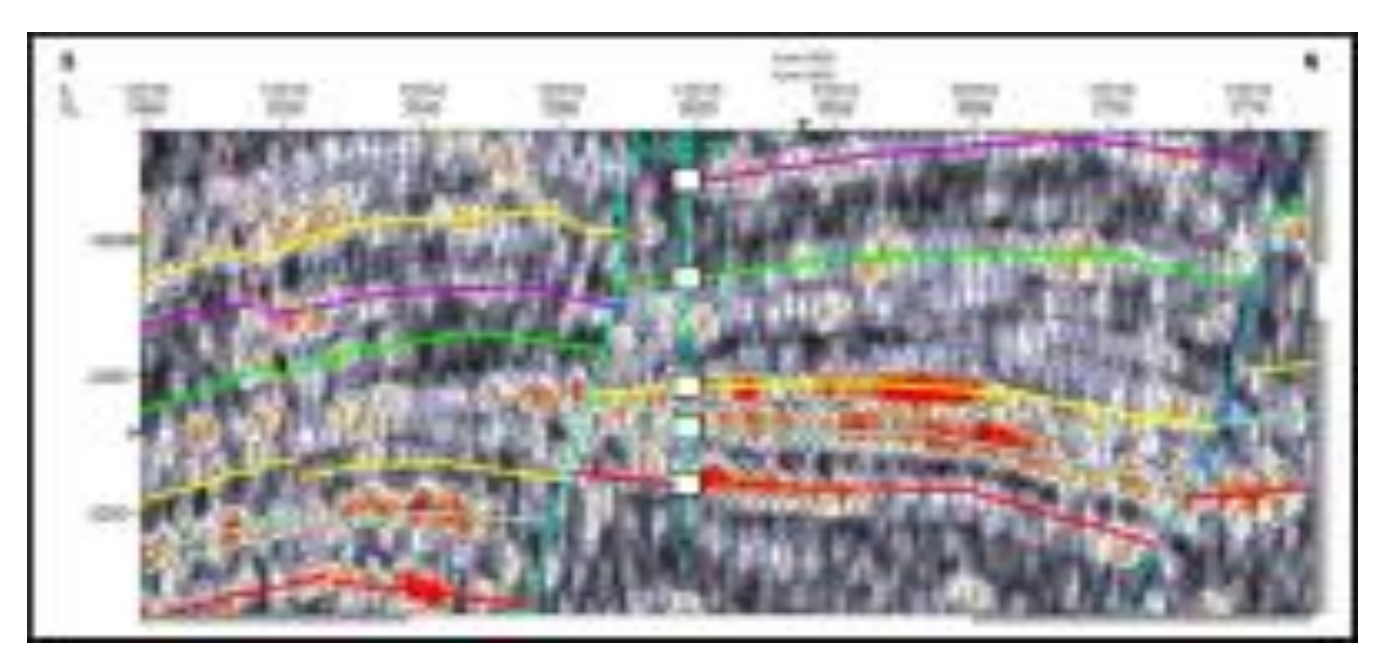


Fig. 14: A cross section through well Nko 31 ST1 revealing reservoirs containing hydrocarbon

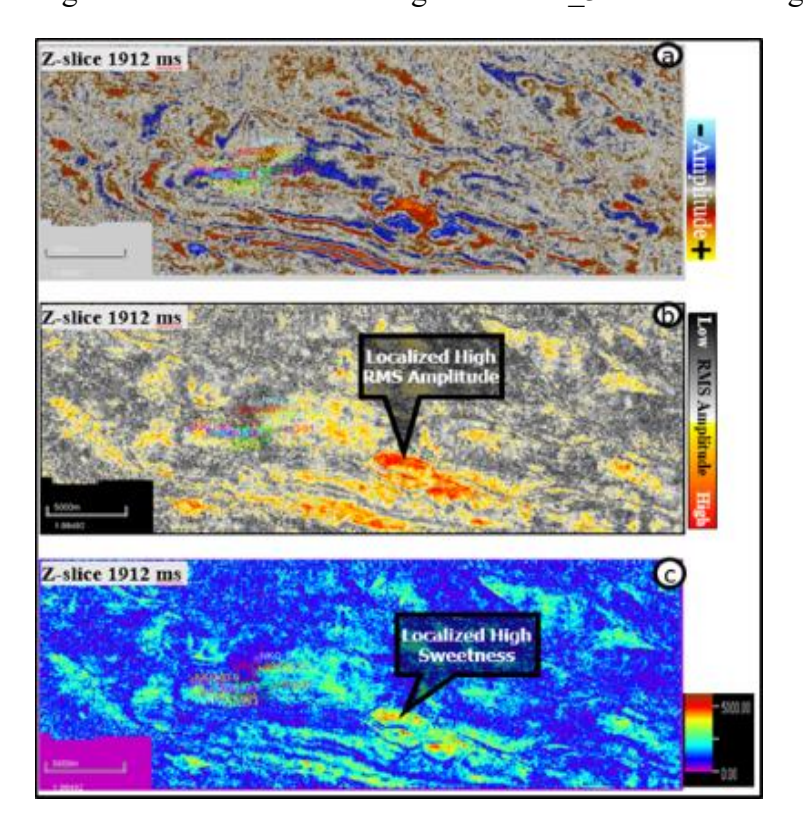


Figure 15: (a) Original seismic time slice at 1912ms showing anomalous high amplitudes. (b) RMS Amplitude time slice at 1912ms showing anomalously high amplitudes corresponding to zones with bright spots. The



anomalous amplitude zones observed in the original seismic time slice show consistent localized high RMS Amplitudes. (c) Shows localized sweetness values corresponding to zones of localized high RMS Amplitudes, indicating the possible extent of porous sands filled with possible reservoir fluids.

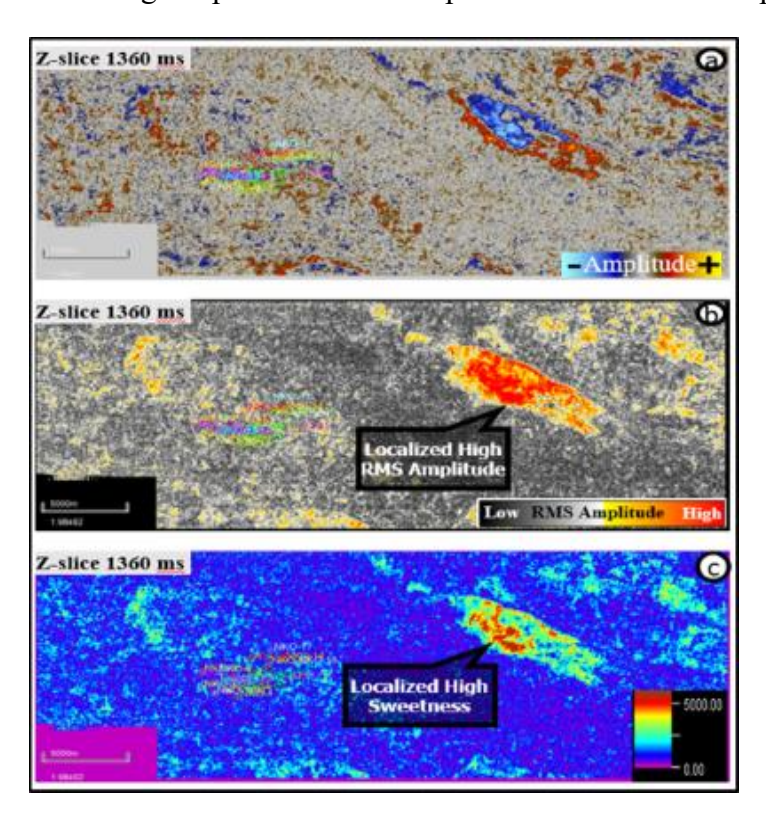


Figure 16: (a) Original seismic time slice at 1360ms showing anomalous high amplitudes. (b) RMS Amplitude time slice at 1360ms showing anomalously high amplitudes corresponding to zones with bright spots. The anomalous amplitude zones observed in the original seismic time slice show consistent localized high RMS Amplitudes. (c) Shows localized sweetness values corresponding to zones of localized high RMS Amplitudes, indicating the possible extent of porous sands filled with possible reservoir fluids.

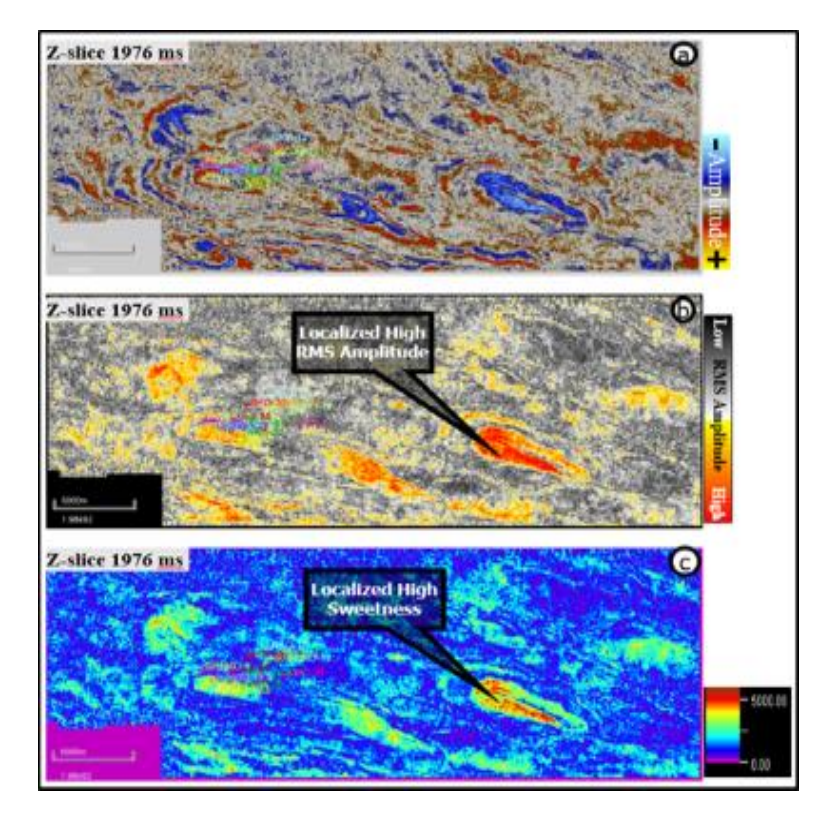


Figure 17: (a) Original seismic time slice at 1976ms showing anomalous high amplitudes. (b) RMS Amplitude time slice at 1976ms showing anomalously high amplitudes corresponding to zones with bright spots. The

anomalous amplitude zones observed in the original seismic time slice show consistent localized high RMS Amplitudes. (c) Shows localized sweetness values corresponding to zones of localized high RMS Amplitudes, indicating the possible extent of porous sands filled with possible reservoir fluids.

Two groups of volume attributes were used; structural (variance edge, 3D edge enhancement, and 3D curvature), and basic attributes (RMS amplitude, envelop, and sweetness), as shown in (Figures 18) to 22. In Figures 18, 19, and 20, the variance edge, 3D edge enhancement, and 3D curvature attributes respectively at time slice -2000ms display discontinuities with high values related to faults. The interpreted faults were inserted into the sliced which tailored perfectly well with regions of high attribute values. Basic attributes; RMS amplitude sweetness attributes (figures 21 and 22). These attributes display regions with potentially high porosity and permeability and saturated with fluid that are structurally embedded by faults.

As illustrated in Figures, 19, and 20, these structural attributes were extracted at a time slice of -2000ms and displayed discontinuities with high values that are closely related to faults. The variance edge attribute (Figure 18) effectively highlighted areas of significant change in the seismic data, which are often indicative of faults or other structural features. Similarly, the 3D edge enhancement attribute (Figure 19) and 3D curvature attribute (Figure 20) provided further insight into the structural configuration of the area. To validate the interpretation, the identified faults were inserted into the time slice, and they correlated well with regions of high attribute values. This integration of structural attributes with fault interpretation enabled a more accurate understanding of the subsurface geology and the role of faults in controlling hydrocarbon accumulation.

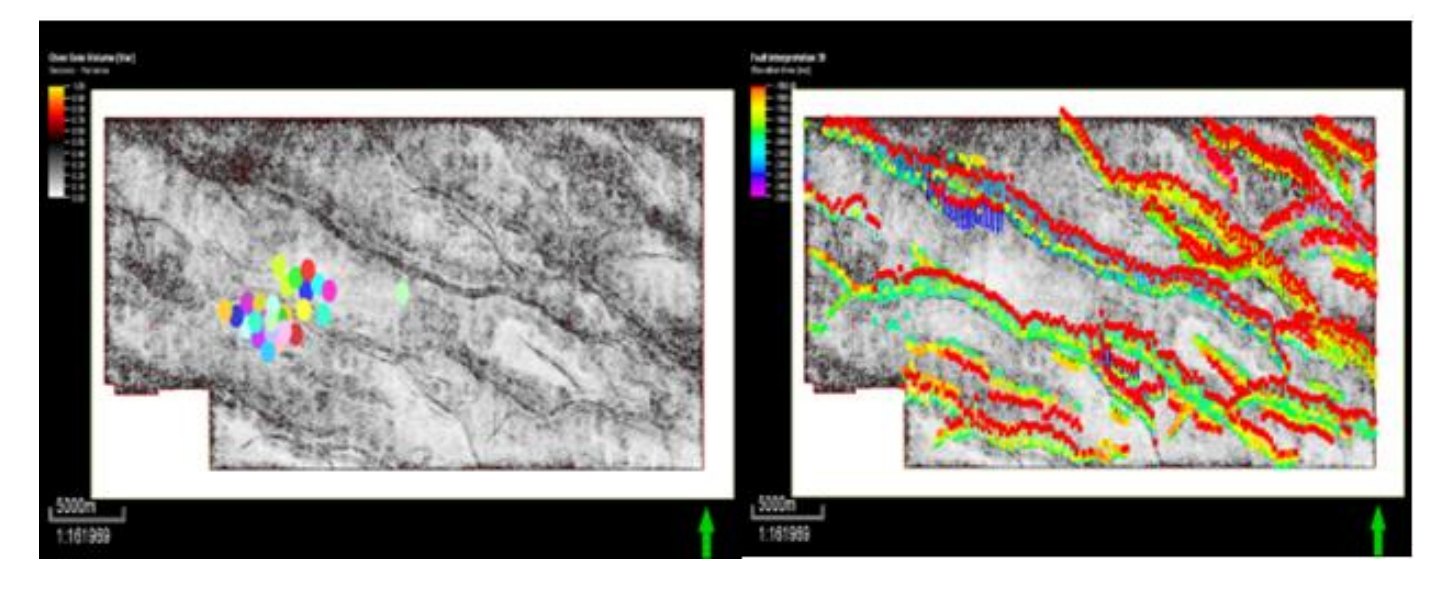


Figure 18: variance-edge attributes showing uninterpreted and interpreted faults

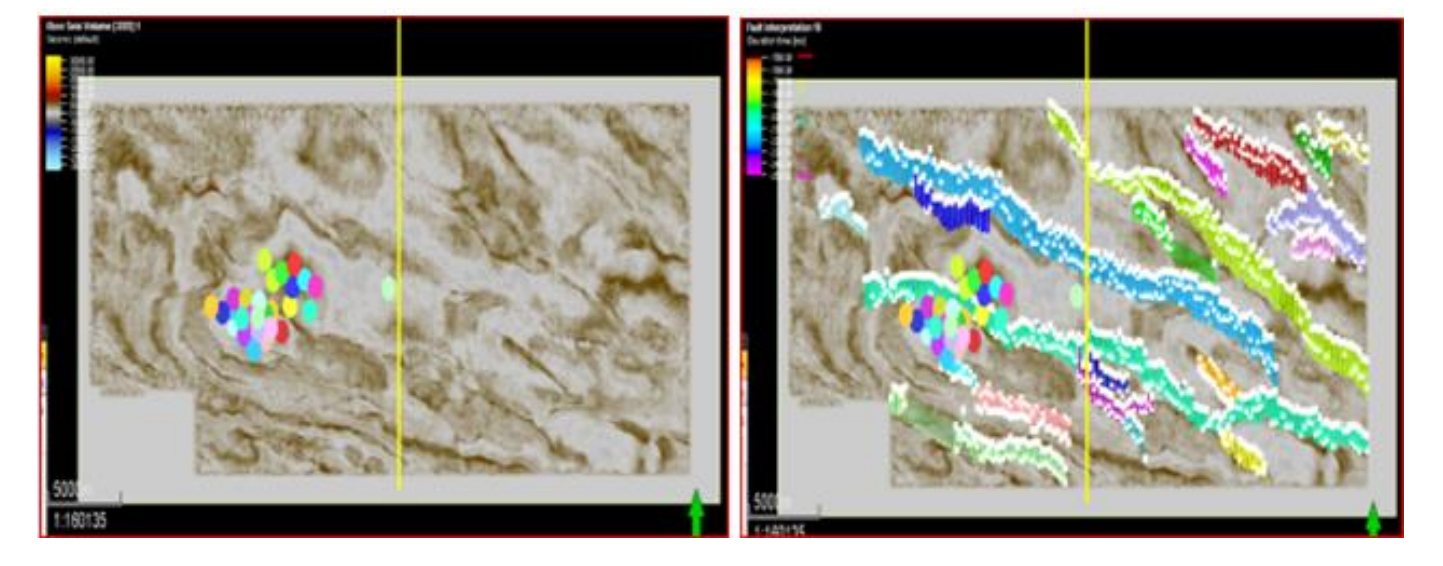


Figure 19: sweetness attributes showing uninterpreted and interpreted faults

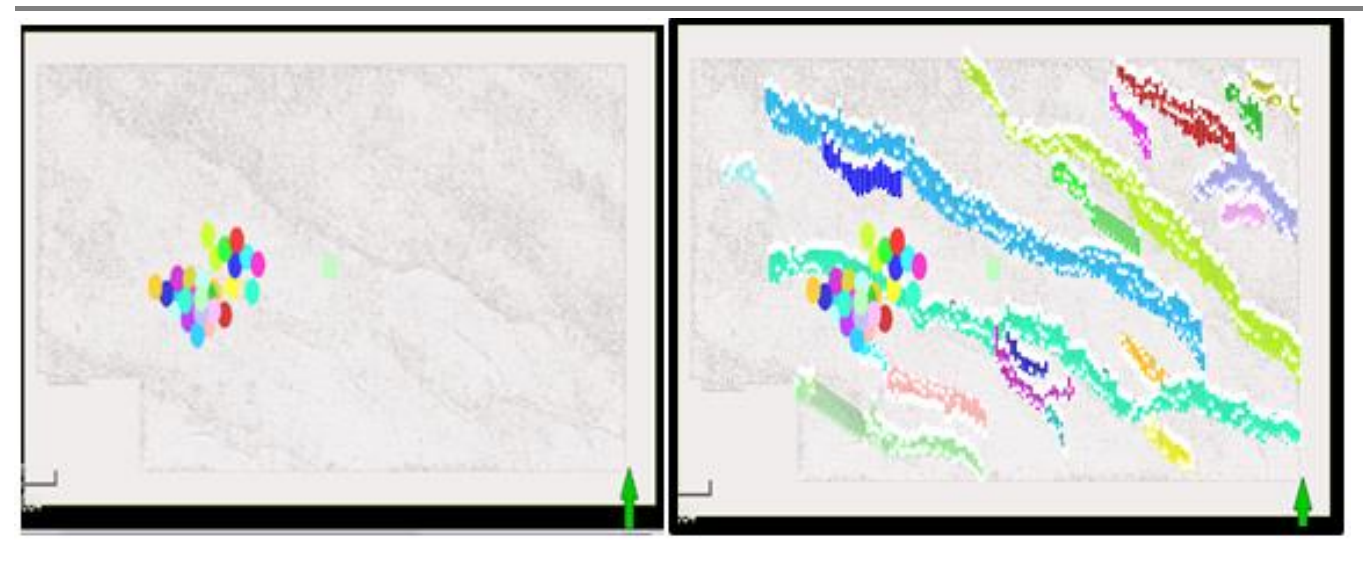


Figure 20: phase attributes showing uninterpreted and interpreted faults

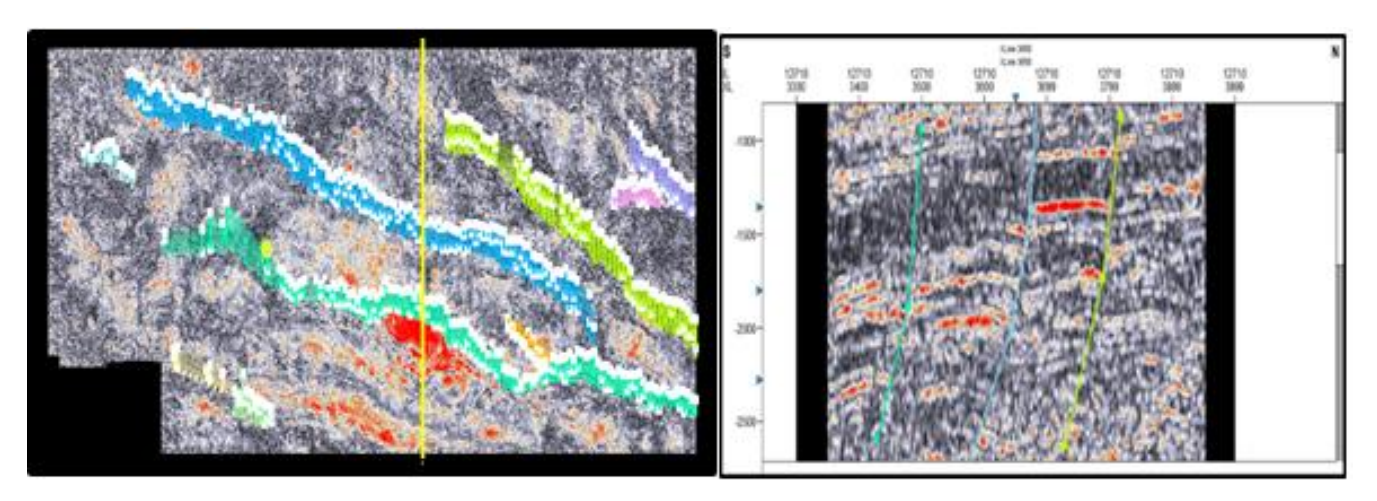


Figure 21: showing how bright spot are structurally and stratigaphically enclose

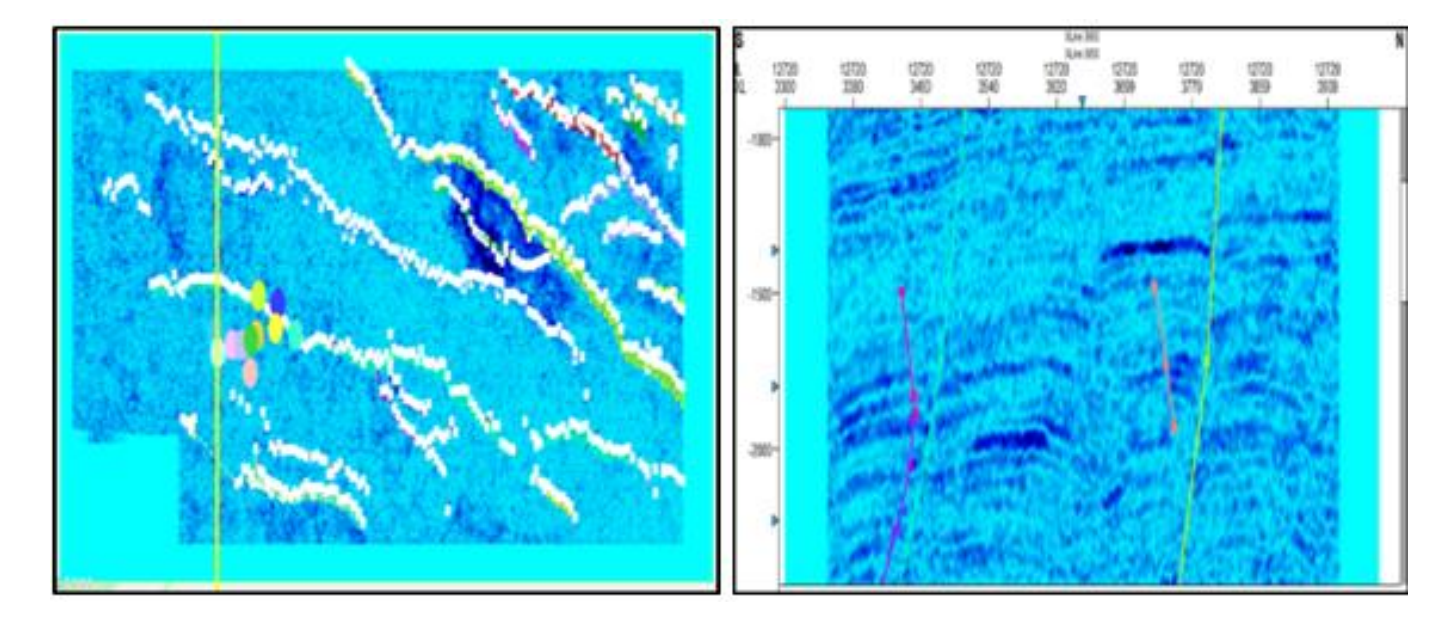


Figure 22: Showing how Bright Spot are structurally and Stratigraphically Enclose

Velocity Model

Velocity model serves as a critical tool for converting seismic interpretation from the time domain to the depth domain. While the seismic data is recorded and interpreted in time due to its measurement in record time,





geologic structures like faults and horizons inherently exist in the depth domain together with well data. To integrate these interpretations with well data and other geological, petrophysical, and production information converting time-based seismic interpretation to depth is essential. Depth conversion helps to mitigate structural uncertainties that can arise from limitations in seismic acquisition and processing. For this study, a polynomial method was employed to construct the velocity model, enabling a more accurate translation of seismic data into the depth domain for comprehensive analysis (figure 23).

Following horizon interpretation and fault mapping, the next step involves converting the seismic travel times to depth values for the acoustic waves. The conversion of time to depth is crucial for generating a reliable curve for well-to-seismic ties and further geophysical analysis. Equation 1 outlines the parameters and equation used to create the velocity model using Petrel software application. The reservoirs of interest are typically located between 847ms and 7482ms on average, although in the southern area, the reservoir package extend up to 748ms. After generating the velocity model, the reservoir was converted to the depth domain, ranging from approximately 4857ms to 5857ms on average, geologic structures are initially interpreted in the time domain on seismic sections but are then converted to depth domain during geologic model creation using the velocity model. This conversion helps eliminate structural uncertainties inherent in the time domain and ensures the geologic structures align with their actual depth. The velocity model was generated using the least square method, calibrated with checkshot data from well Nko_31. The resulting velocity models were non-linear, specifically second order polynomial function.

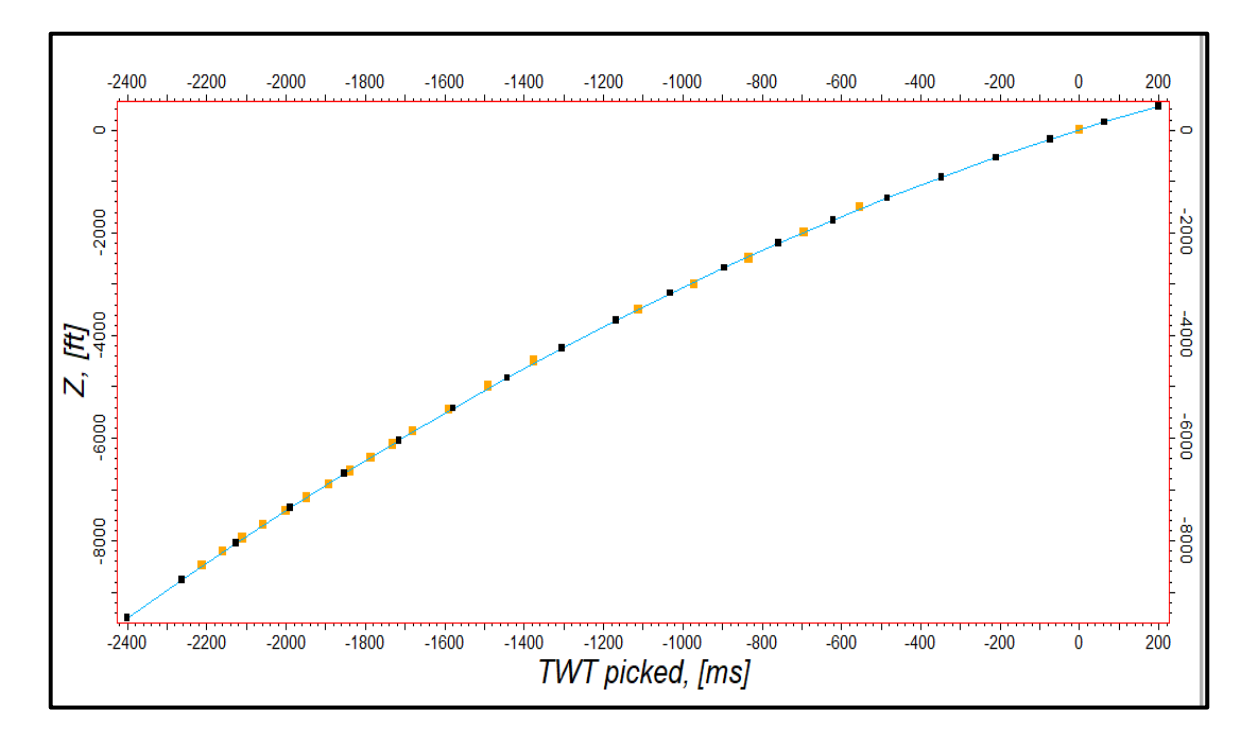


Figure 23: Second-Order Non-Linear Function used for depth conversion

 $Y = 1.98865 + 2.4306X - 0.000636351X^2 \dots 1$

Reservoir Surface Time-Depth Structural Maps

The time surface map of Res_2 reservoir surface demonstrates a complex structural pattern. The time surface map of the reservoir was generated through the interpolation of isochrones, connecting points of equal two-way time to create a contoured surface that defines the structural configuration of the reservoir. The mapped time structure ranges from a minimum of -1107ms, is indicative of structural highs, to a maximum of -2138ms, corresponding to structural lows. A color-coded scale was applied to the structural map, calibrated with values providing visual guidance: red denotes structural highs (shallowest points) and purple represent structural lows (deepest points) as shown in figure 24. Subsequently, a second-order polynomial function was employed to convert time surface map to depth structure map, enabling accurate depth conversion and structural interpretation. The faults network is prominently displayed on both time and depth structural maps, demarcated by dark lines that delineate the complex framework. The depth map exhibits a substantial depth range of 5014

Ft (9093-4079 Ft), with a structural high reaching as shallow as -4079 ft. and structural lows plunging to 9093 ft., underscoring the significance vertical variability in the reservoir's geometry (Figure 25). Notably, the wells in this region were strategically targeted at structural grabens, indicating a deliberate exploration approach to tap potential hydrocarbon accumulation within these down-dropped fault blocks.

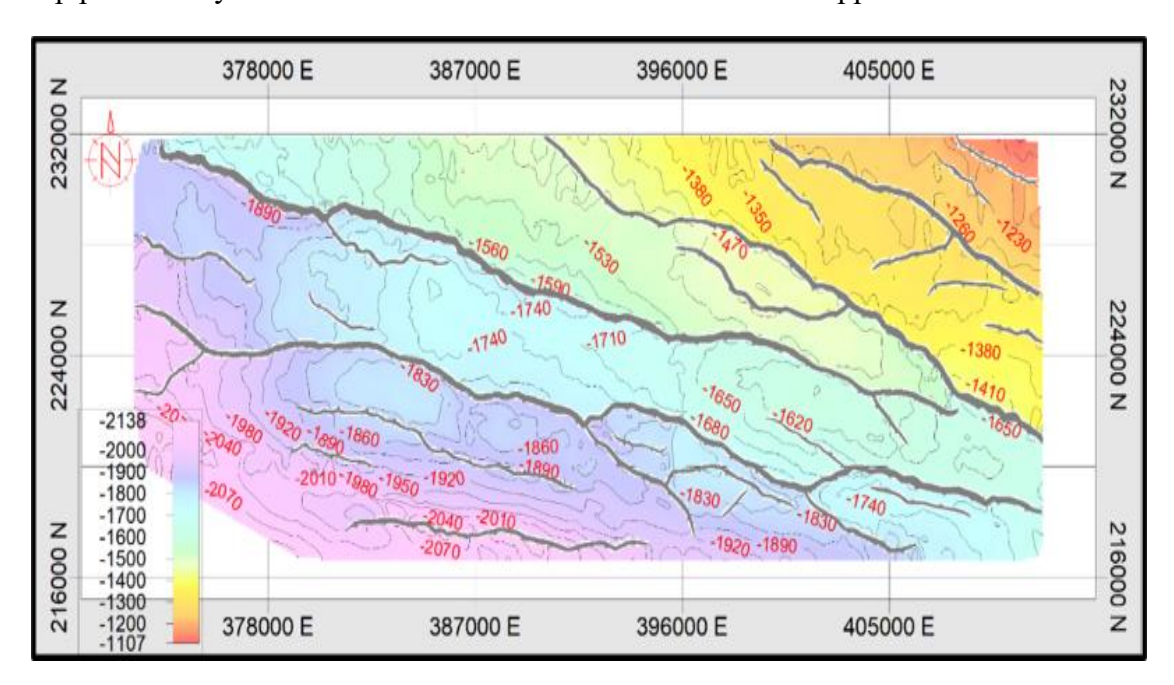


Figure 24: Res 2 Time Surface Structural Map

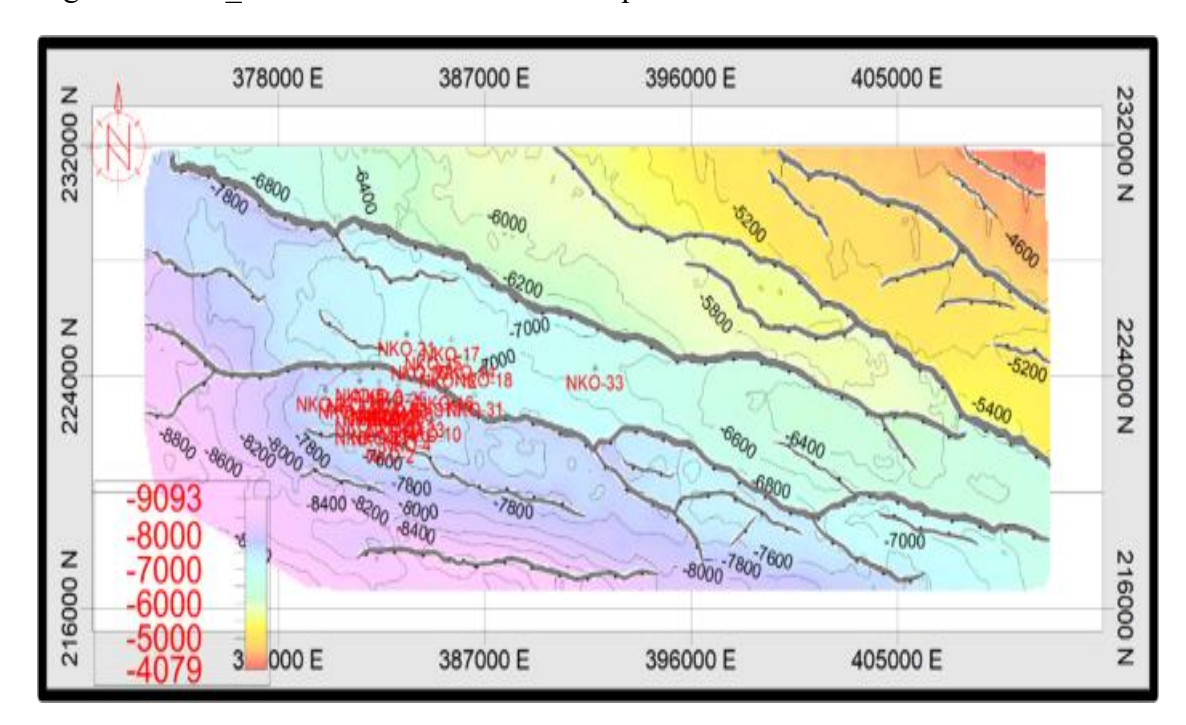


Figure 25: Res 2 Depth Reservoir Structural Map

Res 2 Reservoir Surface Attributes

For the Res_2 reservoir surface, various surface attributes were extracted, including average envelope, extracted value, minimum amplitude, RMS amplitude, sum of magnitude, and upper loop area. The results showed similar patterns across all attributes, with clusters of bright amplitudes predominantly located in the southwestern part of the study area, where most wells were drilled due to confirmed hydrocarbon presence, as evident from well log data in Figure 26 Notably, the bright amplitudes are scattered and correspond to sandy facies, indicating porous and permeable regions that are potential hydrocarbon-bearing zones, highlighting the significance of these attributes in identifying potential hydrocarbon reservoirs.



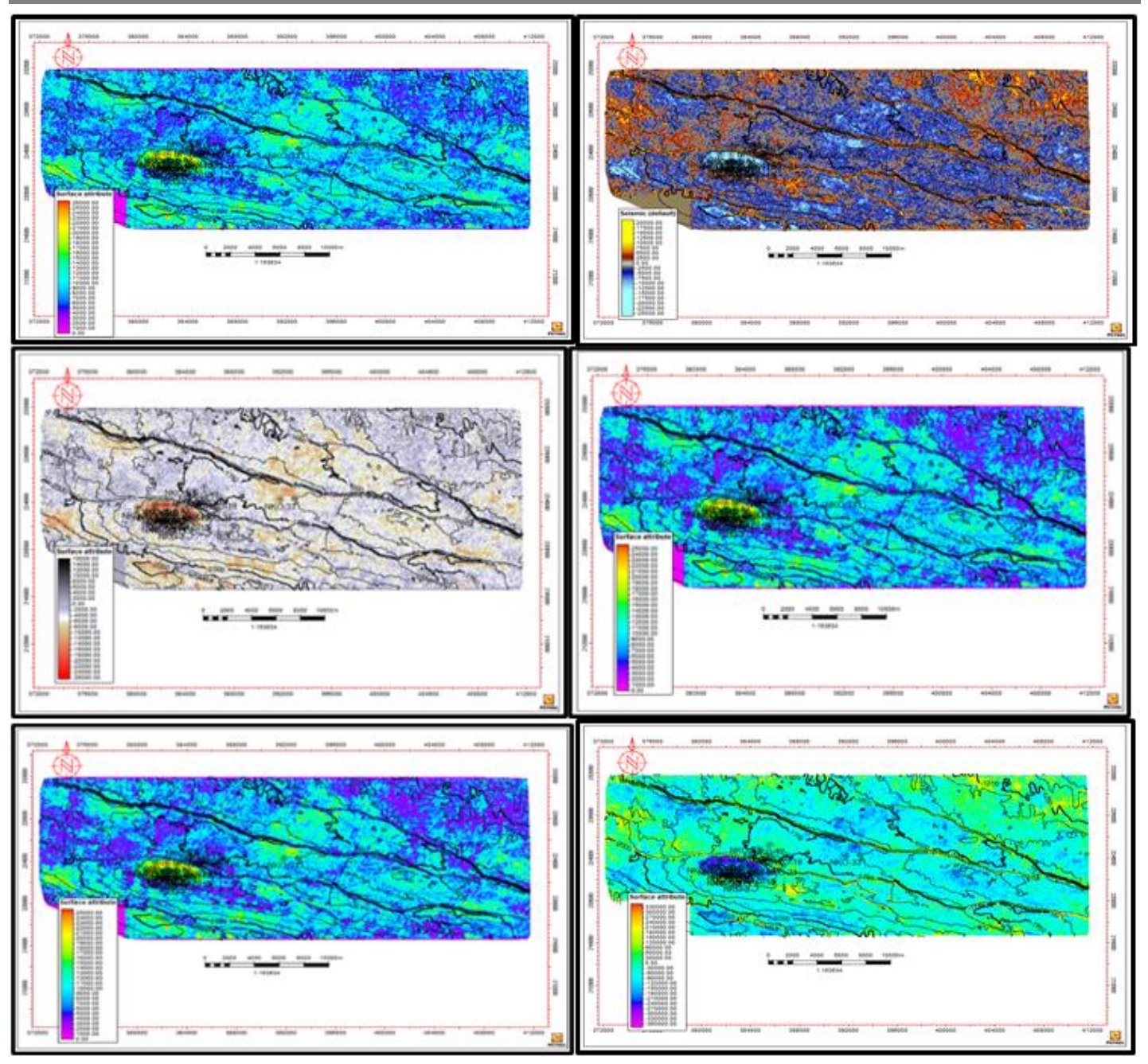


Figure 26: (A) Average Envelop, (B) Extracted Value, (C) Minimum Amplitude, (D) RMS Amplitude, (E) Sum of Magnitude And (F) Upper Loop Area.

CONCLUSION

From structural interpretation, a total of 42 faults, categorized into two groups based on orientation (NE-SW and NW-SE), were identified and mapped on the seismic data. These faults played crucial roles in shaping the field's structure and influencing hydrocarbon migration and accumulation. The faults identification was enhanced with structural attributes, including variance edge, 3D enhancement, and 3D curvature. They are mainly collapse crest and minor relay faults, serving as seals and migrating paths (leaks) at different places

Volume attributes, such as RMS amplitude, average envelope, and sweetness attributes, proved valuable in identifying subtle changes in seismic response due to variations in structure, stratigraphy, lithology, porosity, and hydrocarbon presence. Surface attributes extracted from time structural maps of the reservoir unit revealed bright amplitudes in both drilled and undrilled regions, suggesting potential hydrocarbon prospects.

These findings demonstrate the effectiveness of using multi-seismic Attribute Algorithms in reservoir characterization, enabling more accurate identification and evaluation of potential reservoir rocks.



ISSN No. 2454-6194 | DOI: 10.51584/IJRIAS | Volume X Issue X October 2025

REFERENCE

- 1. Ahaneku, C. V., Okoro, A. U., Odoh, B. I., Anomneze, B.D. O., Chima, K. I., Ejeke, C. F., and Okoli, I. N., (2016). Sequence Stratigraphy, Structural framework and hydrocarbon migration of Ariki field, Nigeria. Petroleum Exploration and Development, 43(1), p.82-88.
- 2. Ali, K., Rahim, K. (2022). Acoustic, density, and seismic attribute analysis to aid gas detection and delineation of reservoir properties. doi: 10.1016/B978-0-323-85465-8.00007-8
- 3. Ajakaiye D. E. and Bally A. W., 2002. Some structural styles on reflection profiles from Offshore Niger Delta. Search and discovery Article. #10031.
- 4. Amit, R., Rajeshwaran, D., Saravana, D., Siddharth, B. (2023). Machine Learning Assisted Fracture Network Characterization of a Naturally Fractured Reservoir Using Seismic Attributes. doi: 10.2118/216965-ms
- 5. Anderson, F. C., and Pedro, A.C.O. (2021). An integrated approach for reservoirs characterization: A case study from the Barreirinhas basin in Maranhão, Brazil. Journal of South American Earth Sciences, doi: 10.1016/J.JSAMES.2021.103610
- 6. Aniefiok, E.I; Udo, J.I, Margaret, U.I, Sunday, W.P (2013) "Petroleum Exploration and production: Past and present Environmental Issues in the Nigeria's Niger Delta". American Journal of Environmental Protection. Vol.1, No.4, 78-90
- 7. Doust, H., and E. Omatsola, 1990.NigerDelta, in J. D. Edwards and P. A. Santogrossi, (eds.); Divergent/passive margin basins: AAPG Memoir 48, p. 239-248.
- 8. Evamy, B.D., Haremboure, J., Kammerling, R., Knaap, W.A., Molloy, F.A., and Rowlands, P.H., 1978. Hydrocarbon habitat of Tertiary Niger Delta, America Association of Petroleum Geologists, Bulletin, v. 62, p. 1-39.
- 9. Kumar, Dhananjay. (2023). Seismic AVO analysis for reservoir characterization. Developments in structural geology and tectonics, doi: 10.1016/b978-0-323-99593-1.00002-1
- 10. Nwaezeapu, V.C., Okoro, A.U., Akpunonu, E.O., Ajaegwu, N.E., Ezenwaka, K.C., Ahaneku, V.A. (2017). Sequence Tratigraphy Approach to Hydrocarbon Exploration: A Case Study Chiadu field Et Eastern Onshore Niger Delta Basin, Nigeria. Journal of Peroleum.
- 11. Nyeneime, O., Etuk., Mfoniso, U., Aka., Okechukwu, A., Agbasi., Johnson, C., Ibuot. (2020). Evaluation of seismic attributes for reservoir characterization over Edi field, Niger delta, Nigeria using 3d seismic data. doi: 10.14419/IJAG.V8I2.31043.
- 12. Obiadi, I., Okoye, F.C., Obiadi, C.M., Irumhe, P., Omeokachie, A.I. (2019). 3-D structural and seismic attribute analysis for field reservoir development and prospect identification in Fabianski Field, onshore Niger delta, Nigeria. Journal of African Earth Sciences Volume 158, October 2019, 103562
- 13. Oumarou, Sanda., Djeddi, Mabrouk., Tabod, Charles, Tabod., Tabod, Charles, Tabod., Jean, Marcel., Simon, Ngos., Jean, Marcel, Abate, Essi., Joseph, Kamguia. (2021). Seismic attributes in reservoir characterization: an overview. Arabian Journal of Geosciences, doi: 10.1007/S12517-021-06626-1.
- 14. Owen, J. (2024). Reservoir Characterization and Performance Analysis Using Type Curves: A Case Study from South-Eastern Bangladesh.
- 15. Reijers, T.J. A., Petters, S. W. and Nwajide, C. S., 1997. The Niger Delta basin. *In*: R.C. Selley, (Ed.); African basins, Amsterdam, Elsivier science, sedimentary basins of the world; Vol. 3, p. 151-172.
- 16. Sofolabo, A.O., A., F., Nwakanma. (2022). Reservoir characterization using integrated seismic attributes and petrophysical parameters in an onshore field of Niger delta basin. International journal of advanced geosciences, doi: 10.14419/ijag.v10i1.31972
- 17. Taner, M. T., Koehler, F. Sheriff, R. E. Complex seismic trace analysis. Society of Exploration Geophysicists GEOPHYSICS 44 (6), 1041-1063, 1979-06